

Systematic Tailoring of Water Absorption in Photopolymerizable (Meth)Acrylate Networks and Its Effect on Mechanical Properties

Nishant Lakhera,¹ Kathryn E. Smith,² Carl P. Frick¹

¹Department of Mechanical Engineering, University of Wyoming, Laramie, Wyoming 82071

²Department of Research and Development, MedShape, Inc. Atlanta, Georgia 30318

Correspondence to: N. Lakhera (E-mail: nishantlakhera@gmail.com)

ABSTRACT: Photopolymerizable (meth)acrylate networks offer several advantages as biomedical materials including their ability to be formed *in situ*, fast synthesis rates, and tailorable material properties. The objective of this study was to identify how phosphate buffered saline (PBS) absorption affects the thermomechanical properties of a ternary (meth)acrylate network. Copolymers consisting of 2-hydroxyethyl (meth)acrylate (2HEMA), benzyl acrylate (BZA), and poly(ethylene glycol) dimethacrylate (PEGDMA; $M_n \sim 750$) were synthesized under UV with varying weight ratios of 2HEMA to BZA. Each composition underwent dynamic mechanical analysis, tensile strain-to-failure testing, Fourier Transform Infrared (FTIR) analysis, and swelling measurements after 24-h immersion in PBS. Networks with higher 2HEMA concentrations absorbed larger amounts of PBS resulting in a larger decrease in the glass transition temperature. PBS absorption affects the mechanical properties of BZA-2HEMA-PEGDMA networks in a manner dependent upon the amount of PBS absorbed into the network. © 2012 Wiley Periodicals, Inc. *J. Appl. Polym. Sci.* 000: 000–000, 2012

KEYWORDS: glass transition; copolymers; mechanical properties; photopolymerization

Received 19 April 2012; accepted 21 July 2012; published online

DOI: 10.1002/app.38371

INTRODUCTION

Photopolymerizable (meth)acrylate-based polymer networks have gained much attention in recent years due to their ability to be formed *in situ*, fast synthesis rates, and simple one-step processing into complex geometries.^{1,2} These properties make these materials particularly advantageous for biomedical applications.^{3–5} For example, their ability to be cured *in vivo* has prompted their use as injectable dental fillings and bone cement.⁶ In addition, the thermo-mechanical properties of (meth)acrylate networks can be readily tailored through changes in copolymer chemistry.^{1,7} The broad range of achievable mechanical properties enables their use in various material platforms ranging from hydrogels^{3,8} to biodegradable networks⁸ to shape-memory polymers.^{9,10} For example, the glass transition temperature (T_g) of a (meth)acrylate based shape-memory polymer can be tuned such that shape recovery initiates in the proximity to the body temperature (37°C);^{11,12} whereas, the force applied upon activation can be tuned by controlling the cross-linking density of the network.^{5,9,10,13} To date, photopolymerizable (meth)acrylate networks have also been proposed for cardiovascular, orthopedic, and drug delivery applications.^{5,14,15}

Depending on the specific application, polymer networks must exhibit certain mechanical properties to serve their designated

function. For example, a polymer used as a shape-memory soft-tissue fixation device must possess a high modulus (10–50 MPa) to allow for high strength deployment into a stiff tissue like bone.^{9,16} On the other hand a soft tissue replacement material must have a modulus that matches the modulus of the host tissue that it is replacing (0.1–100 MPa depending on the tissue), to avoid a mechanical mismatch between the synthetic material and the biological tissue causing injury to the tissue.^{16–18} For applications like cardiovascular stenting or implantation into readily deformable areas like tendons, materials that can undergo very high deformation before failure, are required.^{5,19}

Due to the viscoelastic nature of copolymer networks, their mechanical properties, including strain to failure (ϵ_f) and toughness, depend on the environmental temperature.^{20,21} For example, maximum toughness and failure strain can be achieved by tailoring the copolymer chemistry such that the T_g falls just above body temperature.^{22,23} Previous work has shown that this relationship between T_g and mechanical properties is affected by immersion in PBS in a manner dependent upon the initial viscoelastic state of the polymer.²⁴ For example, in a network that is in a viscoelastic state, the temperature by which peak toughness occurs will shift to a lower temperature under aqueous conditions, indicative of T_g decreasing due to water absorption.

However, high-swelling polymers that exhibit rubbery behavior experience a significant drop in mechanical properties.

It has previously been suggested that the amount of water absorption into the network will dictate how the mechanical properties of copolymer networks are altered in solution.^{16,23} However, to date, a direct relationship between the extent of water absorption and subsequent change in mechanical properties is yet to be established. To the author's best knowledge no previous study has attempted to systematically tailor the polymer system to control the water absorbed into the networks and then characterize the thermomechanical properties using dynamic mechanical analysis. Understanding the mechanical behavior in relation to polymer hydrophilicity is particularly important in biomedical applications when the material is exposed to aqueous environments. Furthermore it is important to ascertain whether the T_g -toughness relationship previously established upholds at varying levels of hydrophilicity. The purpose of this study was to systematically vary the amount of phosphate buffered saline (PBS) absorbed into a (meth)acrylate copolymer network and evaluate its effect on the thermo-mechanical properties. Ternary copolymer networks containing a crosslinker, hydrophilic, and hydrophobic linear monomers were synthesized at varying weight ratios of the hydrophilic and hydrophobic components. Dynamic mechanical analysis (DMA) was performed to evaluate the effect of water absorption on the thermo-mechanical properties of the networks. Stress-strain testing was performed at different temperatures under dry and soaked conditions, spanning the T_g of the networks. FTIR spectroscopy was also performed on the networks to gain insight into the state of absorbed water molecules and changes in chemical structures. The networks were tested under dry conditions and after soaking in PBS solution for 24 h. The results from this study demonstrate that the effect of PBS absorption on the mechanical properties of photopolymerizable networks depends on the extent of water absorption and the binding state of the absorbed water molecules. The networks containing high concentration of hydrophilic monomer absorbed more PBS resulting in a decrease in mechanical properties. The networks with high hydrophobic monomer concentration on the other had absorbed less PBS and thus experienced small change in mechanical properties.

EXPERIMENTAL

Materials

The linear chain builders, benzyl acrylate (BZA; $M_n \sim 162$) which is hydrophobic and 2-hydroxyethyl methacrylate (2HEMA; $M_n \sim 130$) which is hydrophilic were procured from Alfa Aesar. The crosslinker, poly(ethylene glycol) dimethacrylate (PEGDMA; $M_n \sim 750$), and the photoinitiator 2,2-dimethoxy-2-phenylacetophenone (DMPA) were procured from Sigma Aldrich. The materials were used in their as received conditions without any further purification. The names, abbreviations, chemical structures, and molecular weights of all the constituents can be found in Figure 1.

Polymer Synthesis

Ternary polymer networks were formulated using PEGDMA crosslinker, BZA and 2HEMA linear chain builders and 0.5 wt

% of the DMPA photoinitiator. A constant amount (10 wt %) of PEGDMA was used while the weight ratio of BZA to 2HEMA was systematically varied. The compositions of the developed ternary networks chosen for further testing are presented in Table I. Polymer solutions were made by mixing 10 wt % PEGDMA crosslinker and the appropriate amounts of BZA and 2HEMA monomers in a glass vial. All solutions were mixed thoroughly by hand for 30 s followed by 5 min in an ultrasonic shaker (Branson 2510) to ensure a well-distributed solution. The BZA-co-PEGDMA-co-2HEMA networks were then synthesized by free-radical polymerization. For DMA, the polymer solution was injected in between two glass slides separated by glass spacers. For tensile tests sample fabrication, polymer solution was injected in a dogbone-shaped Teflon mold (according to dimensions specified in ASTM D638-03) sandwiched between two glass slides. The dog bone samples were ~ 3 mm wide and 3 mm thick with a gauge length of 20 mm. Either Rain-X or polydimethylsiloxane (PDMS, Dow Corning Sylgard 184) was used on the glass slides as a release agent, depending on the network. The specimens were polymerized under a UV lamp (Blak Ray Model B 100 A/R) for 30 min. After polymer synthesis, all polymer samples were placed in an oven at 90°C for 1 h.

PBS Absorption

For samples tested under wet conditions, PBS solution was prepared by dissolving one PBS tablet (Sigma Aldrich; #P4417) in 200 mL distilled water. Test specimens were immersed in the solution for 24 h. The weight of the sample was recorded before (W_i) and after soaking it in PBS (W_f). The PBS content (W_{PBS}) of each composition after 24 h was accordingly calculated using the following equation^{24,25}:

$$W_{\text{PBS}} = \frac{W_f - W_i}{W_i}$$

Dynamic Mechanical Analysis

DMA was performed to characterize the low-strain thermo-mechanical properties of the networks using a TA Instruments Q800 DMA. Samples were cut into small rectangles and lightly sanded with coarse grit sandpaper to remove any surface imperfections. Prior to testing the soaked specimens were coated with vacuum grease (Dow Corning High-Vacuum Grease) to prevent any loss of water absorbed by the networks. Each sample was tested under tensile loading with the sample dimensions measuring approximately 25.0 x 5.0 x 1.0 mm³. The samples were thermally equilibrated at -50°C for 5 min and heated to 200°C at a constant rate of 5°C/min while subjected to a 0.1% dynamic strain at 1 Hz. The ratio of loss modulus to the storage modulus, $\tan \delta$, was plotted as a function of temperature. The T_g was defined as the peak of $\tan \delta$.²⁶ The onset of glass transition, T_{on} , was calculated using an intersecting line method at the initial drop in glassy modulus, where the starting point of the left tangent line was $T_g - 50^\circ\text{C}$ and the starting point of the right tangent line was the T_g . The Universal Analysis software package was used to determine exact values of T_g and T_{on} . Duplicate tests were run for each composition under both dry and wet conditions to ensure repeatability.

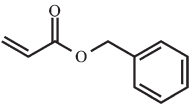
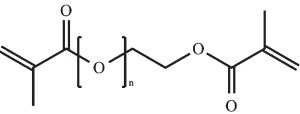
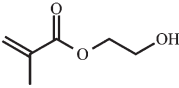
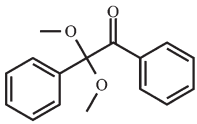
Material	Structure	Molecular Weight (g/mol)
Benzyl Acrylate (BZA)		162.19
Poly(ethylene glycol) dimethacrylate (PEGDMA)		750
2-Hydroxyethyl methacrylate (2HEMA)		130.14
2,2-Dimethoxy-2-phenylacetophenone (DMPA)		256.32

Figure 1. Names, abbreviations, chemical structure, and molecular weights of all constituents used.

Tensile Strain to Failure Testing

Tensile strain-to-failure testing was performed on dogbone samples using a MTS hydraulic load frame (MTS 858 Mini Bionix II) equipped with a MTS 651 environmental chamber, a liquid nitrogen cooling mechanism and a laser extensometer (MTS LX 500). The edges of the samples were sanded to remove any defects or imperfections. Samples were loaded onto tensile grips and equilibrated in the thermal chamber for 20 min to ensure thermal equilibrium. Samples soaked in PBS solution were coated with vacuum grease prior to loading them onto the tensile grips. The initial effective gauge length of the samples was defined by placing reflective laser tape at the two ends of the gauge section, and the displacement was recorded by the laser extensometer. All samples were deformed at a strain rate of 5%/min until fracture occurred. Only the samples that broke in their gauge lengths were considered for further calculations. The strain at fracture, determined from the displacement recorded by the laser extensometer, was defined as strain to failure, ϵ_f and the corresponding stress was defined as stress at failure, σ_F . Toughness of the samples in MJ/m^3 was calculated as area under the stress–strain curve. Each composition was tested at five different temperatures spanning from T_g to 40°C below T_{on}

under dry and soaked conditions. Five tests were run at a particular temperature for each composition to ensure repeatability.

Fourier Transform Infrared Spectroscopy

The chemical structure of the networks was analyzed by performing Fourier transform infrared spectroscopy in attenuated total reflectance (ATR) mode using a Bruker Vector 22 with a PIKE MIRacle ATR module and ZnSe crystal. The 16 scans were obtained at 1 Hz on dry samples and samples immersed in PBS for 24 h. Prior to obtaining spectra, wet samples were patted lightly to remove bulk water on the surface and immediately placed on the crystal. Peak wavenumbers were identified using the Essential FTIR software. Three samples were scanned per condition.

RESULTS

PBS Content

The PBS absorption of the five copolymer networks tested in this study are presented in Table I. The 0 wt % BZA-100 wt % 2HEMA samples demonstrated maximum PBS absorption after 24 h of soaking of approximately 27 wt %. PBS content decreases with increasing BZA concentration down to 2 wt %. This is expected as BZA is relatively hydrophobic of the two linear builders.

Dynamic Mechanical Analysis

Representative storage modulus vs. temperature and tan delta vs. temperature curves for 20 wt % BZA-80 wt % 2HEMA and 80 wt % BZA-20 wt % 2HEMA under both dry and soaked conditions as obtained for DMA analysis are shown in Figure 2(a,b), respectively. As shown in Figure 2(a), under dry testing conditions both compositions experience a significant drop in the storage modulus with an increase in temperature, and the modulus plateaus out at higher temperatures. Such behavior is characteristic of a lightly crosslinked polymer network.²⁷ After soaking in PBS for 24 hours the same general shape of the storage modulus curve is observed. For the 80 wt % BZA-20 wt % 2HEMA curve the limited water absorption does not dramatically affect the glass transition behavior. For the 20 wt % BZA-80 wt % 2HEMA material, the glass transition decreases significantly, and the rubbery modulus of the 20 wt % BZA-80 wt % 2HEMA network increased compared with dry conditions. But this effect was not observed with the 80 wt % BZA-20 wt % 2HEMA network. Figure 2(b) displays the tan delta as a function of temperature for the same two compositions. For the 20 wt % BZA-80 wt % 2HEMA network, the height of the tan δ peak at T_g decreased after 24 hours in PBS; whereas, PBS had

Table I. Names, Thermo-Mechanical Properties and PBS Absorption of All Compositions

Name	wt % BZA- wt % 2HEMA	T_g ($^\circ\text{C}$) Dry	T_g ($^\circ\text{C}$) soaked	PBS absorption after 24 h (W_{PBS})
90 wt % 2HEMA-co-PEGDMA	0-100	115.1 ± 1.2	16.6 ± 2.8	0.27 ± 0.05
18 wt % BZA-co-2HEMA-co-PEGDMA	20-80	101.3 ± 6.7	18.8 ± 4.1	0.08 ± 0.04
45 wt % BZA-co-2HEMA-co-PEGDMA	50-50	67.0 ± 1.4	51.9 ± 2.2	0.03 ± 0.01
72 wt % BZA-co-2HEMA-co-PEGDMA	80-20	37.5 ± 3.3	33.6 ± 1.1	0.01 ± 0.01
90 wt % BZA-co-PEGDMA	100-0	25.3 ± 2.5	21.1 ± 1.6	0.02 ± 0.00

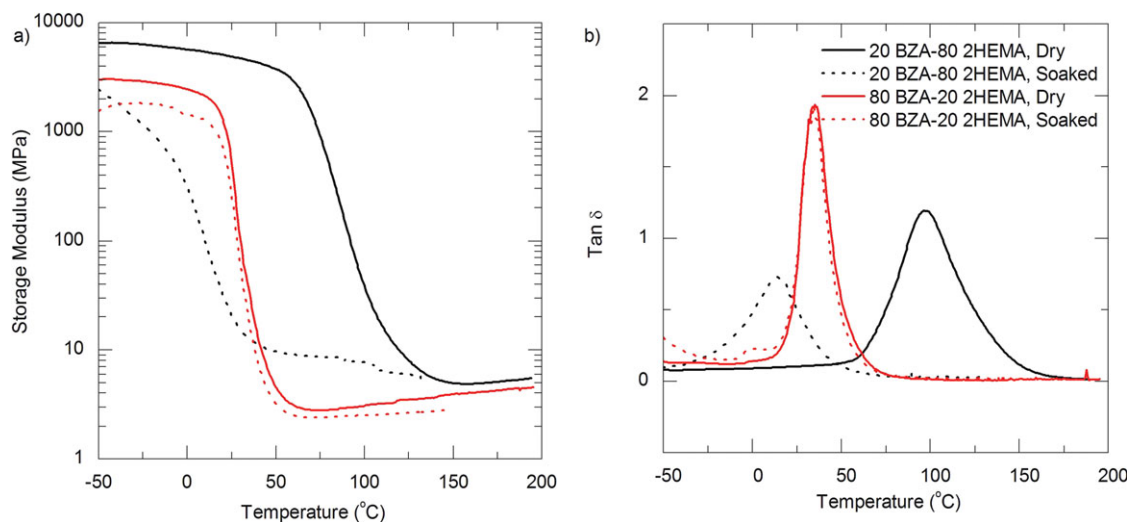


Figure 2. (a) Storage modulus vs. temperature curve for 20 wt % BZA-80 wt % 2HEMA and 80 wt % BZA-20 wt % 2HEMA samples for both dry and soaked conditions. (b) Tan delta vs. temperature curves for the same. [Color figure can be viewed in the online issue, which is available at wileyonlinelibrary.com.]

little effect on the $\tan \delta$ behavior for the 80 wt % BZA-20 wt % 2HEMA network.

The measured T_g s for each composition are shown in Table I. Under dry conditions, the T_g of 80 wt % BZA-20 wt % 2HEMA network is lower as compared with 20 wt % BZA-80 wt % 2HEMA network, 37.5°C as compared with 101.3°C. The shape of the $\tan \delta$ curve under dry condition changes from short and wide to tall and narrow from 20 wt % BZA-80 wt % 2HEMA to 80 wt % BZA-20 wt % 2HEMA network. Soaking the networks in PBS for 24 h had a significant effect on 20 wt % BZA-80 wt % 2HEMA samples. The T_g of this network was significantly reduced under soaked condition as represented by the shift towards the left in storage modulus and $\tan \delta$ curves as a function of temperature. For example, 20 wt % BZA-80 wt % 2HEMA samples under dry conditions exhibited a T_g of 101.3°C, while the T_g got reduced to 18.8°C under soaked conditions. On the other hand, 80 wt % BZA-20 wt % 2HEMA samples experienced only a minor decrease in the T_g value from 37.5 to 33.6°C, when tested under soaked conditions.

The effect of water absorption on T_g of all networks tested as a function of wt % BZA is presented in Figure 3. Under dry conditions, increasing BZA concentration caused a decrease in the T_g of the networks. At low BZA concentrations (0–40 wt %), immersion in PBS caused a significant decrease in the T_g of the networks compared with dry conditions. At BZA concentrations greater than 50%, PBS absorption had a negligible effect on T_g compared with dry conditions, with T_g continuing to decrease as more BZA was added. As can be seen from Figure 3, 80 wt % and 100 wt % BZA networks have almost the same T_g under dry and soaked conditions, while 0 wt % BZA networks had a difference of about 100°C in their T_g under dry and soaked conditions.

Stress–Strain Behavior

To study the effect of PBS content on the thermomechanical behavior of copolymer networks, tensile strain-to-failure testing

was performed at different temperatures spanning the glassy and viscoelastic regimes, including each copolymer's T_g and T_{on} . The representative stress–strain curves obtained for 20 wt % BZA-80 wt % 2HEMA under dry and soaked conditions are shown in Figure 4(a,b), respectively. Figure 4(c,d) represents similar curves for 80 wt % BZA-20 wt % 2HEMA samples. Under dry conditions the stress–strain behavior of both networks transitions from viscoelastic to rubbery as the testing temperature approaches T_g . For temperatures below T_{on} both

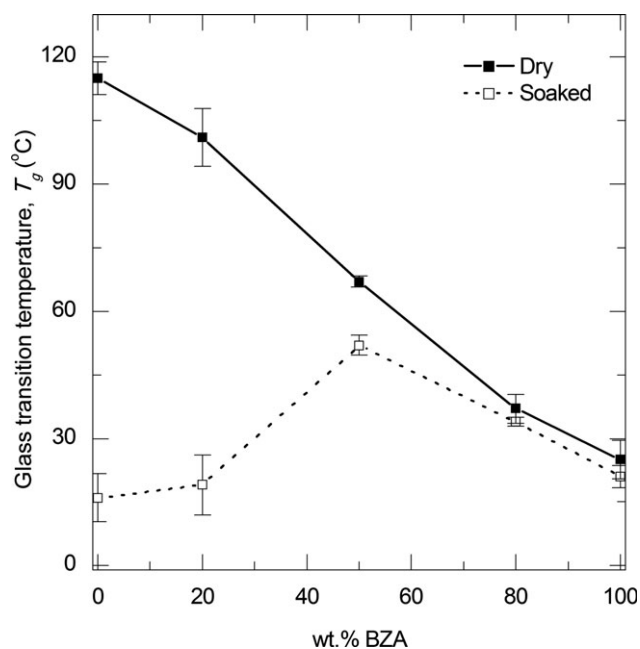


Figure 3. T_g as a function of wt % BZA as obtained from the DMA analysis performed on selected compositions as mentioned in Table I. The T_g is observed to decrease with the increase in wt % BZA. For the same wt % BZA the T_g obtained was less for soaked samples as compared with the dry ones.

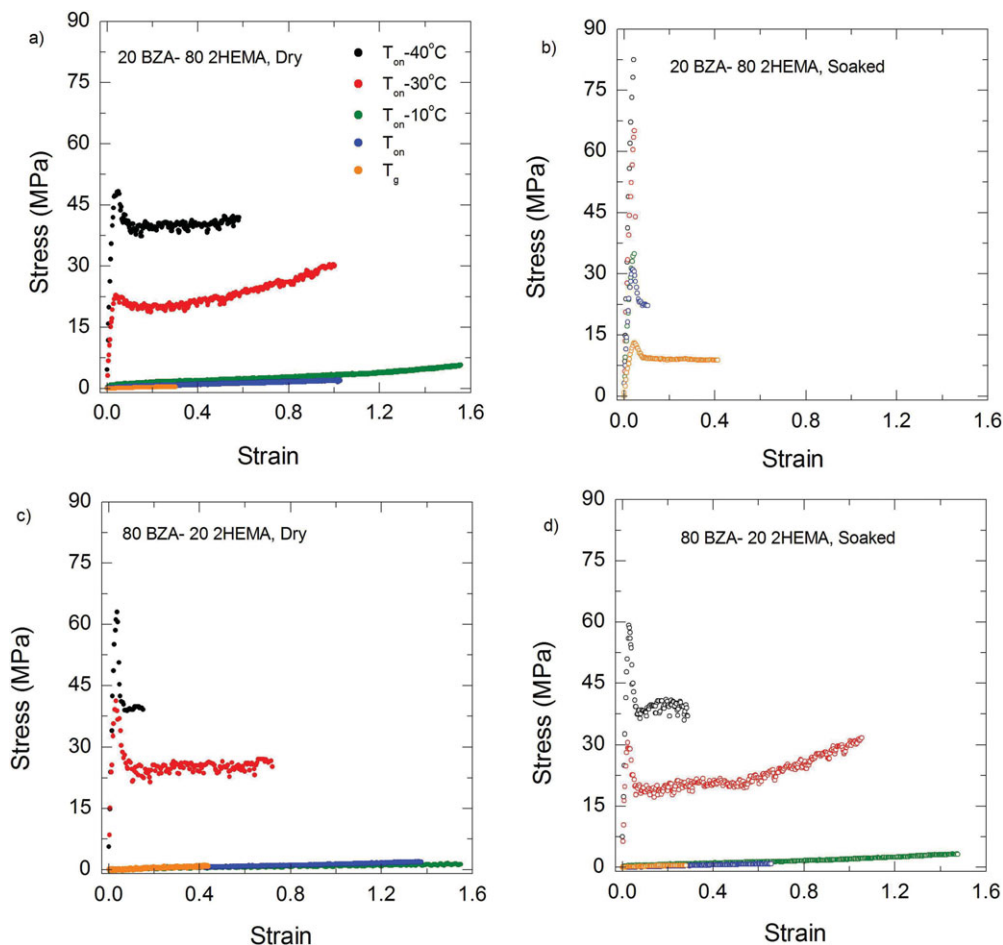


Figure 4. (a) Stress–strain curve for 20 wt % BZA-80 wt % 2 HEMA samples tested under dry conditions. (b) Same composition tested under soaked condition. (c) Stress–strain curve for 80 wt % BZA-20 wt % 2HEMA samples tested under dry conditions. (d) Same composition tested under soaked condition. [Color figure can be viewed in the online issue, which is available at wileyonlinelibrary.com.]

networks demonstrated an initial linear elastic response, followed by a yield point and then strain hardening. When the testing temperature approached T_g , the stress–strain response became linear elastic, indicative of a rubbery state. All networks demonstrated analogous behavior under dry conditions for all testing temperatures. After 24 h in PBS, the effect of temperature on the stress–strain response differed for each composition. The 20 wt % BZA-80 wt % 2HEMA samples demonstrated an increase in strain as the testing temperature increased above T_{on} [Figure 4(b)]. However, the overall strain capacity was reduced by almost 75% compared with dry conditions. The 80 wt % BZA-20 wt % 2HEMA samples tested under soaked conditions however, demonstrated similar transition in stress–strain behavior as observed under dry conditions [Figure 4(d)].

Effect of Composition on Mechanical Properties

Using the results obtained from the stress–strain testing under dry and soaked conditions, σ_B , ϵ_f and toughness were plotted as a function of the difference between the testing temperature (T) and T_g of each composition (i.e., $T - T_g$). Figure 5(a,b) shows σ_F as a function of $T - T_g$ for all networks tested under dry and soaked conditions, respectively. In general, σ_F increased with

decrease in testing temperature, independent of dry or soaked testing. Maximum σ_F was observed at the lowest testing temperature. The trend observed in σ_F was also independent of the network composition. For testing under dry conditions for all networks, maximum σ_F observed at the lowest testing temperature was in the range of 30–45 MPa, while values in the range of 20–35 MPa were observed when the tests were performed under soaked conditions. For soaked testing, 20 wt % BZA-80 wt % 2HEMA samples presented an exception by demonstrating higher σ_F values for all testing temperatures. The maximum σ_F observed at lowest temperature for this network was around 80 MPa.

Figure 6 represents ϵ_f as a function of $T - T_g$. As shown in Figure 6(a) for all compositions tested under dry conditions, the ϵ_f increased as a function of temperature to a maximum and then decreased as the testing temperature approached T_g . The temperature at which maximum ϵ_f occurred varied from 25 to 40°C below T_g depending on the network composition. In general, the maximum values of ϵ_f were in the range of 130–150% for all compositions. Low wt % 2HEMA compositions demonstrated a similar trend under immersion in PBS, as shown in

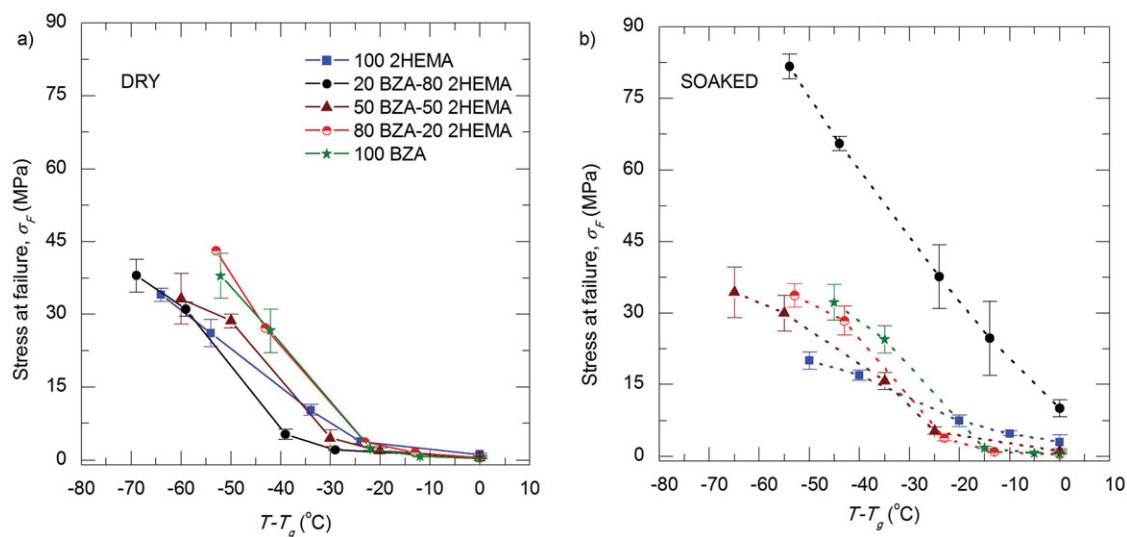


Figure 5. (a) Stress at failure as a function of testing temperature for dry tested samples of all composition and (b) shows the stress at failure as a function of testing temperature for the soaked condition tests. [Color figure can be viewed in the online issue, which is available at wileyonlinelibrary.com.]

Figure 6(b). However, for higher wt % 2HEMA, i.e. 20 wt % BZA- 80 wt % 2HEMA and 0 wt % BZA-100 wt % 2HEMA compositions, no peak in ϵ_f is observed. These compositions demonstrate very low ϵ_f increasing from 5 to 30% as the testing temperature approached T_g . Samples tested at T_g exhibited the lowest ϵ_f independent of the network composition.

Toughness of the networks was calculated from the stress–strain curves produced in Figure 4 and plotted as a function of $T - T_g$ (Figure 7). Under dry conditions, all compositions followed a similar trend observed in ϵ_f reaching a maximum in toughness at temperatures ranging 40–60 $^{\circ}\text{C}$ below T_g . These maximum toughness values ranged from 15 to 28 MJ/m^3 with the 50 wt % BZA-50 wt % 2HEMA and 20 wt % BZA-80 wt % 2HEMA compositions exhibiting the highest levels of toughness.

Under soaked conditions, the relationship between temperature and toughness was dependent on the network composition. For high wt % BZA networks, a maxima in toughness was observed at the same temperatures observed under dry conditions for the same composition. However, at lower BZA concentrations (i.e., 20 wt % BZA-80 wt % 2HEMA and 0 wt % BZA-100 wt % 2HEMA), toughness remained low at all testing temperatures on the order of 1–5 MJ/m^3 under soaked conditions as compared with values for dry tests (on the order of 1–21 MJ/m^3). For all other compositions, the toughness values under dry conditions are slightly higher than those observed under soaked conditions. For example, 50 wt % BZA-50 wt % 2HEMA samples exhibit a maximum toughness value of 28 MJ/m^3 when tested under dry conditions, while a value of 20 MJ/m^3 was observed when tested under soaked condition.

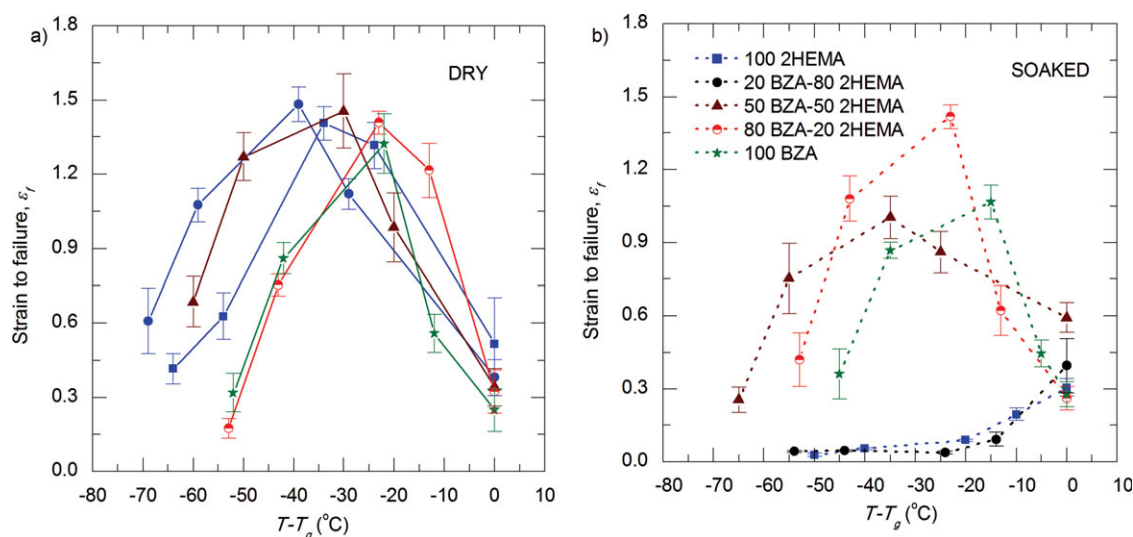


Figure 6. (a) Strain to failure as a function of testing temperature for dry tested samples of all composition and (b) shows the strain to failure as a function of testing temperature for the soaked condition tests. [Color figure can be viewed in the online issue, which is available at wileyonlinelibrary.com.]

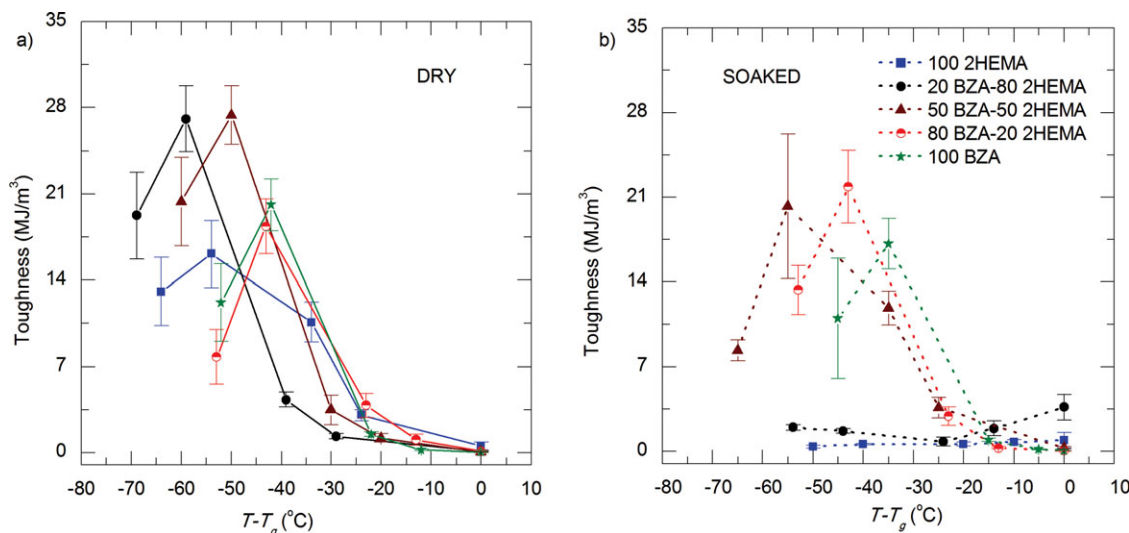


Figure 7. (a) Toughness as a function of testing temperature for dry tested samples of all composition and (b) shows the toughness as a function of testing temperature for the soaked condition tests. [Color figure can be viewed in the online issue, which is available at wileyonlinelibrary.com.]

Fourier Transform Infrared Spectroscopy

FTIR-ATR was performed on select compositions to identify any possible mechanisms related to changes in intermolecular bonding due to PBS absorption. Representative spectra for the 80 wt % BZA-20 wt % 2HEMA, 50 wt % BZA-50 wt % 2HEMA, and 20 wt % BZA-80 wt % 2HEMA are shown in Figure 8. The peaks at 1070–1080 cm^{-1} , 1730 cm^{-1} , and 2950 cm^{-1} correspond to the C–O–C stretching vibrations, C=O stretching vibration, and C–H stretching vibrations (for the methyl and benzyl groups), respectively. After immersion in PBS, peaks appear around 1650–1700 cm^{-1} and 3400–3600 cm^{-1} corresponding to O–H bending and stretching vibrations of the water molecules, respectively. The intensity of these peaks increases with decreased BZA concentration indicating increased hydrogen bond formations. The shifts in the O–H stretching and O–H bending bands to lower frequencies at lower BZA concentrations are also indicative of more hydrogen bond formations between adjacent water molecules and/or water molecules with polymer chains.²⁸ A slight decrease in intensity in the C–O–C vibrational bands under wet conditions is observed for all compositions most likely due to the formation of hydrogen bonds between the ethylene glycol groups on the crosslinker and surrounding water molecules. However, a decreased intensity of the C=O bands was only observed for the 50 wt % BZA-50 wt % 2HEMA and 20 wt % BZA-80 wt % 2HEMA compositions [Figure 7(a)] suggesting that an increased number of phenyl ring side chains (from the BZA monomer) prevents some water binding to this polar group.²⁹

DISCUSSION

The objective of this study was to evaluate the effect of water content on the thermo-mechanical behavior of a photopolymerizable (meth)acrylate network. Our results demonstrate that PBS absorption affects the mechanical properties of copolymer networks in a manner dependent upon the amount of PBS absorbed into the networks. Previous work has demonstrated

that the mechanical properties of a copolymer network are highly dependent on the network's T_g in relation to testing temperature.^{16,23} For example, ϵ_f and toughness of (meth)acrylate networks reaches a maxima at a temperature just below T_g . In networks that absorbed small amount of PBS (less than 5 wt %), this toughness maxima has been shown to shift to a lower temperature. This result was attributed to a decrease in T_g causing the material to transition to a different viscoelastic state.²³ In networks that absorb large amounts of water/PBS, the mechanical behavior, including modulus, ϵ_f and toughness have been shown to decrease significantly. It is believed that this drastic drop in properties is due to the breaking of secondary hydrogen bonds among the polymer chains that contribute to

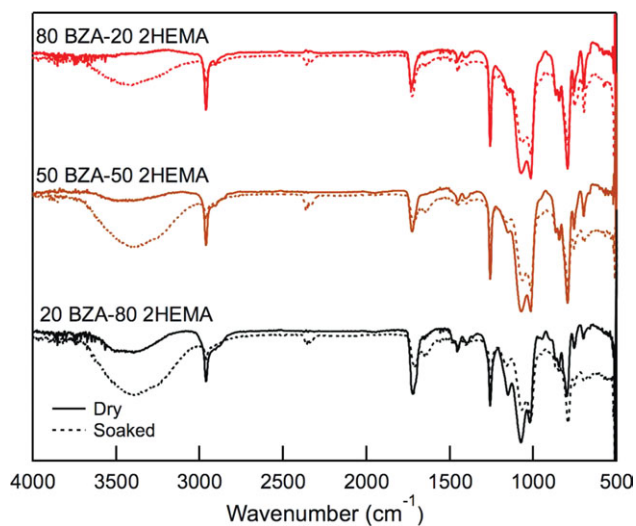


Figure 8. Representative FTIR-ATR spectra for the 20 wt % BZA-80 wt % 2HEMA, 50 wt % BZA-50 wt % 2HEMA, and 80 wt % BZA-20 wt % 2HEMA compositions under dry and soaked conditions. [Color figure can be viewed in the online issue, which is available at wileyonlinelibrary.com.]

polymer rigidity and toughness. In this study, we sought to delineate the effects of PBS caused by plasticization and those caused by water binding.

A ternary copolymer network (BZA-*co*-PEGDMA-*co*-2HEMA) was adopted to allow for the systematic control of network hydrophilicity by varying the weight ratio of BZA to 2HEMA, without changing the crosslinker concentration (PEGDMA). Crosslinking density has been shown to affect water absorption and the mechanical properties, independent of monomer chemistry¹⁶; thus it was important to maintain a consistent crosslinking density for all compositions, as demonstrated by the similar rubbery moduli for all compositions [around 3–4MPa; Figure 2(a)]. The linear monomers, BZA and 2HEMA, were selected because they had side groups with opposing polarities allowing for a systematic change in PBS absorption (Table I). 2HEMA is extensively used in contact lenses and hydrogels^{30,31} and contains highly polar hydroxyl side groups that readily form hydrogen bonds with water molecules.³² On the other hand, BZA contains a bulky benzyl side group which acts as a steric hindrance for water molecules to diffuse into the network.^{33,34} Furthermore, BZA and 2HEMA also have vastly different T_g values, 6 and 120°C, respectively allowing for the T_g of the network to also be systematically tailored by varying their relative ratios, under dry conditions (Table I and Figure 3).

Interestingly, the relative ratio of BZA to 2HEMA had little effect on the stress-strain behavior of the network at different temperatures. Rather, the mechanical properties were strongly dictated by the testing temperature in relation to T_g . Both 80 wt % BZA-20 wt % 2HEMA and 20 wt % BZA-80 wt % 2HEMA networks exhibited a decrease in σ_F as temperature approached T_g as well as a peak in toughness and ϵ_f at a testing temperature 20–30°C below T_g [Figures 5(a), 6(a), and 7(a)], trends previously described for (meth)acrylate copolymer networks.^{23,35} These changes in mechanical properties are attributed to the network transitioning from a glassy to viscoelastic to rubbery behavior as testing temperature approaches T_g . Thus under dry conditions, the copolymer chemistry could be tailored to achieve the mechanical properties desired for a specific application that required certain thermal conditions.

However in the presence of PBS, this relationship between temperature and mechanical behavior becomes dependent on copolymer composition in a manner related to the relative hydrophilicity of the network. Specifically, those compositions that absorbed little PBS (less than 5 wt %) exhibited a change in stress-strain properties as the temperature approached T_g in a manner similar to the trends observed under dry conditions [Figures 4(c,d), and 5]. In contrast, for compositions that absorbed higher amounts of PBS (e.g., 20 wt % BZA-80 wt % 2HEMA), the relationship between temperature and stress-strain behavior was altered in PBS compared with what was observed under dry conditions. Specifically, the networks began to exhibit a brittle stress-strain response below T_g [Figure 4(a,b)], with both ϵ_f and toughness never reaching a peak value but rather decreasing an order of magnitude compared to when tested at the same temperature, in relation to T_g , under dry conditions. This reduction in mechanical properties was partially observed in the 50 wt % BZA-50 wt % 2HEMA samples

but became more pronounced as more 2HEMA was added to the network and the PBS content increased, up to almost 20% for the 0 wt % BZA-100 wt % 2HEMA composition.

The difference in the thermo-mechanical behavior with varying BZA-2HEMA concentrations can be explained if one considers the thermodynamic state of water molecules absorbed. Water molecules can be present in a polymer network in one of two states: bound and/or free. Bound water refers to absorbed water molecules that disrupt the intermolecular hydrogen bonding amongst the polymer chains to form hydrogen bonds with any polar groups along the polymer chains. Water molecules that do not interact with the polymer chains, but rather form hydrogen bonds among themselves and exists in clusters are referred to as free water.^{36,37} Bound water creates a one-phase thermodynamic system with the polymer network, in which T_g becomes dictated by the concentrations and T_g s of the water and individual monomer components.³⁸ Free water content can also affect the T_g of the networks by increasing the intermolecular distance between the chains, thereby weakening the secondary bonding between the chains and allowing the chains to slide relative to each other.³⁴ For the compositions with high BZA concentration, the low PBS content in combination with the evidence of some hydrogen bond formation in the network, as observed with FTIR, (Table I and Figure 8) suggests that the few water molecules absorbed are primarily acting in a bound state and causing an incremental shift in T_g .³⁹ However, as PBS content increases, more free water molecules become present in the network, limiting chain mobility and thus driving the network to a more brittle mechanical state at temperatures below the materials T_g .

This study also sought to evaluate how PBS affects the thermo-mechanical behavior of copolymer networks using DMA. DMA is a useful characterization technique that allows for the evaluation of thermal transitions as well as a simple screening method to determine how temperature affects the mechanical behavior. It is often challenging to assess the transition behaviors of polymers absorbed with moisture if these transitions, such as T_g , occur above 50°C, as the moisture begins to evaporate quickly. The soaked materials tested in this study were coated with vacuum grease to arrest water absorption for intermediate temperatures. Furthermore, the compositions tested in this current study all exhibited T_g values well below 50°C in PBS such that their full glass transition behavior into the rubbery state could be captured. The decreased height and increased breadth of the $\tan \delta$ peak for the 20 wt % BZA-80 wt % 2HEMA composition after PBS immersion suggests that the effective crosslinking density of the network increased due to water binding with the polymer chains and adjacent water molecules.⁴⁰ This effect was not observed for the 80 wt % BZA-20 wt % 2HEMA composition where there was minimal PBS absorption (Table I) and less evidence of water binding from the FTIR (Figure 8).

Our study highlights the importance of considering the degree of hydrophilicity when attempting to enhance the mechanical properties of copolymer networks under aqueous conditions. Previous work has suggested that properties such as ϵ_f and toughness can be enhanced by tailoring the network T_g to fall near the environmental temperature. The results of this study

indicates that this principle holds true for networks that absorb small amounts of moisture (less than 5%). However at larger PBS contents, the increased amount of free water present in the network reduces chain mobility leading to more brittle mechanical behavior. Therefore, in higher swelling polymers alternative methods might need to be considered to enhance the mechanical properties for biomedical applications.

CONCLUSIONS

In this study, the concentrations of a hydrophilic and hydrophobic monomers in a ternary (meth)acrylate network were varied in order to evaluate the systematic effect of PBS absorption on their thermo-mechanical properties under physiological conditions. The relationship between temperature and the mechanical properties of BZA-co-PEGDMA-co-2HEMA networks is affected by PBS absorption to an extent dependent upon the total PBS content. Networks with high 2HEMA concentrations absorbed more PBS resulting in a decrease in mechanical properties independent of the testing temperature in relation to T_g . In contrast, low 2HEMA networks absorbed low amounts of PBS and thus, experienced a small change in mechanical properties, characteristic of the T_g decreasing to a lower temperature. These results suggest that there is a certain range of water absorption where the thermomechanical properties of these networks can be tailored under aqueous conditions using the T_g -temperature shift approach.

ACKNOWLEDGMENTS

The authors thank David Safranski and Haskell Beckham for their assistance with the FTIR testing.

REFERENCES

1. Brey, D. M.; Ifkovits, J. L.; Mozia, R. I.; Katz, J. S.; Burdick, J. A. *Acta Biomater.* **2008**, *4*, 207.
2. Frick, C. P.; Lakhera, N.; Yakacki, C. M. **2011**.
3. Elisseeff, J.; Anseth, K.; Sims, D.; McIntosh, W.; Randolph, M.; Langer, R. *Proc. Natl. Acad. Sci. USA* **1999**, *96*, 3104.
4. Yakacki, C. M.; Gall, K. *Shape-Memory Polymers*; Springer-Verlag Berlin: Berlin, **2010**.
5. Yakacki, C. M.; Shandas, R.; Lanning, C.; Rech, B.; Eckstein, A.; Gall, K. *Biomaterials* **2007**, *28*, 2255.
6. Lovell, L. G.; Lu, H.; Elliott, J. E.; Stansbury, J. W.; Bowman, C. N. *Dent. Mater.* **2001**, *17*, 504.
7. Anseth, K. S.; Bowman, C. N.; BrannonPeppas, L., *Biomaterials* **1996**, *17*, 1647.
8. West, J. L.; Hubbell, J. A. *React. Polym.* **1995**, *25*, 139.
9. Yakacki, C. M.; Shandas, R.; Safranski, D.; Ortega, A. M.; Sassaman, K.; Gall, K. *Adv. Funct. Mater.* **2008**, *18*, 2428.
10. Gall, K.; Yakacki, C. M.; Liu, Y. P.; Shandas, R.; Willett, N.; Anseth, K. S. *J. Biomed. Mater. Res. Part A* **2005**, *73*, 339.
11. Lendlein, A.; Langer, R. *Science* **2002**, *296*, 1673.
12. Lakhera, N.; Laursen, C. M.; Safranski, D. L.; Frick, C. P. *J. Polym. Sci. Part B: Polym. Phys.*
13. Lakhera, N.; Yakacki, C. M.; Nguyen, T. D.; Frick, C. P. *J. Appl. Polym. Sci.*
14. Anseth, K. S.; Metters, A. T.; Bryant, S. J.; Martens, P. J.; Elisseeff, J. H.; Bowman, C. N. *J. Control. Release* **2002**, *78*, 199.
15. Sharma, B.; Williams, C. G.; Khan, M.; Manson, P.; Elisseeff, J. H. *Plast. Reconstr. Surg.* **2007**, *119*, 112.
16. Smith, K. E.; Temenoff, J. S.; Gall, K. *J. Appl. Polym. Sci.* **2009**, *114*, 2711.
17. Lendlein, A.; Kelch, S. *Clin. Hemorheol. Microcirculation* **2005**, *32*, 105.
18. Gloria, A.; Causa, F.; De Santis, R.; Netti, P. A.; Ambrosio, L. *J. Mater. Sci.-Mater. Med.* **2007**, *18*, 2159.
19. Ebara, S.; Iatridis, J. C.; Setton, L. A.; Foster, R. J.; Mow, V. C.; Weidenbaum, M. *Spine* **1996**, *21*, 452.
20. Smith, T. L. *J. Polym. Sci. Part A: General Papers* **1963**, *1*, 3597.
21. Smith, T. L. *Polym. Eng. Sci.* **1965**, *5*, 270.
22. Drummond, J. L. *J. Dental Res.* **2008**, *87*, 710.
23. Smith, K. E.; Parks, S. S.; Hyjek, M. A.; Downey, S. E.; Gall, K. *Polymer* **2009**, *50*, 5112.
24. Smith, K. E.; Trusty, P.; Wan, B.; Gall, K. *Acta Biomater.* **2011**, *7*, 558.
25. Temenoff, J. S.; Athanasiou, K. A.; Lebaron, R. G.; Mikos, A. G. *J. Biomed. Mater. Res.* **2002**, *59*, 429.
26. Cook, W. D.; Delatyck, O. *J. Polym. Sci. Part B-Polym. Phys.* **1974**, *12*, 1925.
27. Mather, P. T.; Luo, X. F.; Rousseau, I. A. *Ann. Rev. Mater. Res.* **2009**, *39*, 445.
28. Kusanagi, H.; Yukawa, S. *Polymer* **1994**, *35*, 5637.
29. Krisanangkura, P.; Packard, A. M.; Burgher, J.; Blum, F. D. *J. Polym. Sci. Part B-Polym. Phys.* **2010**, *48*, 1911.
30. Li, X. M.; Cui, Y. D.; Xiao, J. L.; Lia, L. W. *J. Appl. Polym. Sci.* **2008**, *108*, 3713.
31. Wang, Y. J.; Tan, G. X.; Zhang, S. J.; Guang, Y. X. *Appl. Surf. Sci.* **2008**, *255*, 604.
32. Singh, T. R. R.; McCarron, P. A.; Woolfson, A. D.; Donnelly, R. F. *Eur. Polym. J.* **2009**, *45*, 1239.
33. Barnes, A.; Corkhill, P. H.; Tighe, B. J. *Polymer* **1988**, *29*, 2191.
34. Corkhill, P. H.; Jolly, A. M.; Ng, C. O.; Tighe, B. J. *Polymer* **1987**, *28*, 1758.
35. Yakacki, C. M.; Willis, S.; Luders, C.; Gall, K. *Adv. Eng. Mater.* **2008**, *10*, 112.
36. Hofer, K.; Mayer, E.; Johari, G. P. *J. Phys. Chem.* **1990**, *94*, 2689.
37. Nakamura, K.; Hatakeyama, T.; Hatakeyama, H. *Polymer* **1983**, *24*, 871.
38. Rault, J.; Lucas, A.; Neffati, R.; Pradas, M. M. *Macromolecules* **1997**, *30*, 7866.
39. Pinal, R. *Entropy* **2008**, *10*, 207.
40. Krupicka, A.; Johansson, M.; Hult, A. *Macromol. Mater. Eng.* **2003**, *288*, 108.